Draft version September 22, 2025
Typeset using LaTeX default style in AASTeX631

Radiative Effect of Dust on the Climate of Early Mars
Summer Research Final Report

Yilin Wang[1,2,*] and Robin Wordsworth[2,3]

[1] School of Physics, Peking University, Beijing 100871, China
[2] School of Engineering and Applied Sciences, Harvard, Cambridge, MA 02138, USA
[3] Department of Earth and Planetary Sciences, Harvard, Cambridge, MA 02138, USA

ABSTRACT

The climate of early Mars was likely strongly influenced by dust with optical properties distinct from those of modern Mars due to a more reducing ancient environment. In this work, we develop a modeling framework to investigate the radiative effects of such dust. We couple Mie scattering theory with a 1D radiative-convective model to assess the impact of airborne dust, and we use the Hapke model to analyze the spectral reflectance of surface regolith systematically. The framework is validated against modern Mars conditions. Our analysis then yields a key physical insight: the surface albedo is as sensitive to particle effective radius as it is to the material's intrinsic absorption. This result demonstrates that physical texture is as critical as bulk composition, highlighting that a holistic approach considering mineralogical and physical properties is essential for accurately modeling the climates of early Mars and for the spectral interpretation of rocky exoplanets.

Keywords: Planetary atmospheres(1244) — Planetary climates(2184)

1. INTRODUCTION

Mars is widely known as a red planet, with the reddish color coming from its surface dust containing oxidized iron. Martian dust, as we know it, plays a vital role in the radiative energy budget, thus affecting the climate on present Mars. Therefore, it is hypothesized that dust also played a crucial role in the climate of early Mars. Also, geological evidence has shown that the early Martian environment had been reducing (Liu et al. 2021). This suggests that the radiative effect of dust on early Mars likely differed significantly from that on the modern planet. This motivates us to look closely into the radiative impact of dust on the climate of early Mars.

The radiative effect of dust can be divided into two aspects: the scattering effect of airborne dust and the reflective properties of surface dust, i.e., regolith. The latter aspect led us to investigate further the correlation between the reflectance spectra and the properties of the regolith. This is a problem of fundamental significance and is not confined to the study of early Mars; it has important implications in the field of exoplanet characterization as well.

In this report, we systematically build and validate a modeling framework to investigate these effects. We use Mie theory to compute the optical properties of airborne dust particles (extinction efficiency, single-scattering albedo, and asymmetry parameter). These properties are then integrated into a 1D radiative-convective climate model (PCM_LBL) to simulate their impact on the atmospheric thermal structure. Subsequently, we critically evaluate several theoretical models for surface reflectance, focusing on the Hapke model, to quantify the relationship between the physical properties of regolith, such as particle size and composition, and its spectral albedo. Using this framework, we explore the climate system's sensitivity to key dust parameters, revealing the significant and often under-appreciated role of particle size. Finally, we discuss the inherent limitations of these models and the broader implications of our findings for reconstructing the climate of early Mars and for the spectral characterization of rocky exoplanets.

wylin@stu.pku.edu.cn

rwordsworth@seas.harvard.edu

* Visiting undergraduate research assistant at SEAS

2. MODELING APPROACH AND VALIDATION

2.1. *Refractive Index Data*

The complex refractive index describes the behavior when the material interacts with the electromagnetic field. In this report, we use the notation $m = \sqrt{\varepsilon} = n + ik$, with n, k being the real part and imaginary part of the refractive index, and ε is the relative permittivity.

The refractive index data of basalt is from Pollack et al. (1973) and Lamy (1978), and will be indicated as `pollack` in this report. The refractive index of modern Martian dust is from Haberle et al. (2017), which is retrieved from observation (Wolff et al. 2006, 2009), with additional UV part from Connour et al. (2022), and will be referred to as `wolff`. The refractive index of a volcanic ash sample from Grímsvötn is given by Deguine et al. (2020). The refractive indices of other mineral materials are from the Aerosol Refractive Index Archive of the University of Oxford. The refractive indices used in this report are shown in Fig. 1.

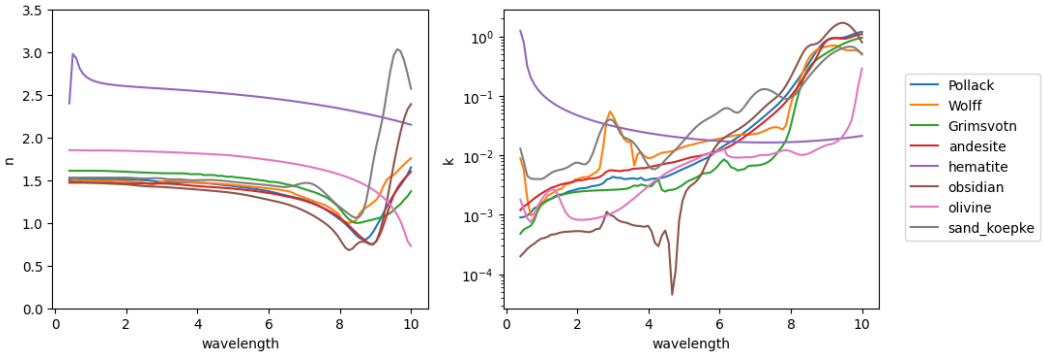

Figure 1. The refractive index of materials used in this project, the left and the right panels show the real and imaginary parts of the refractive index, respectively.

2.2. *Modeling the Radiative Effects of Airborne Dust*

2.2.1. *Mie Scattering*

When light strikes a particle, the radiation field interacts with the medium and results in scattering. The Mie theory solves Maxwell equations with appropriate boundary conditions for homogeneous, spherical particles. When the particle size is much smaller than the wavelength of incident light, the Mie theory degenerates into the Rayleigh scattering limit; when the particle size is much larger than the wavelength, it goes to the geometric optics limit.

The most important result from Mie theory is the scattering properties of a single particle, including the scattering efficiency Q_s, the absorption efficiency Q_a, and the phase function $p(\cos\Theta)$. There are also related quantities including the extinction efficiency $Q_e = Q_s + Q_a$ and the asymmetry parameter $g = \frac{1}{4\pi}\int_0^{2\pi}\int_0^{\pi}\cos\Theta \cdot p(\cos\Theta)\sin\Theta \mathrm{d}\Theta\mathrm{d}\phi$. These quantities describe the interaction of incident light with the spherical particle.

The code to perform Mie scattering calculations is written in Python. The core function `bhmie` is from the website of Pierrehumbert (2010). The code is modified to include particle size distribution, different particle species, and the variation of number density and size parameter with height. The key input of the code is the refractive index of the particles, which is described in section 2.1. The code then outputs the extinction coefficient β, single scattering albedo ϖ, and asymmetry parameter g, which are the most important parameters in multiscattering calculations.

Fig. 2 is an example result of the Mie scattering calculations, it is adapted from Fig. 12.5 in Petty (2004). From the figure, we can see the typical trend of extinction efficiency with respect to the size parameter $x = \frac{2\pi r}{\lambda}$, $Q_e \to 0$ when $x \to 0$, then Q_e oscillates as x increases, until finally approaches $Q_e = 2$ with a large x limit. From the logarithmic scale graph, we can see that the change of particle radius only shifts the curve along the $\log(\lambda/\mu\mathrm{m})$ axis, which is a natural result from the fact that the Mie scattering process depends on only refractive index m and size parameter x. However, this seemingly trivial feature on a logarithmic scale can significantly impact practical problems, as indicated in the linear graph on the right panel. When we focus on the spectral feature within the visible range, the difference

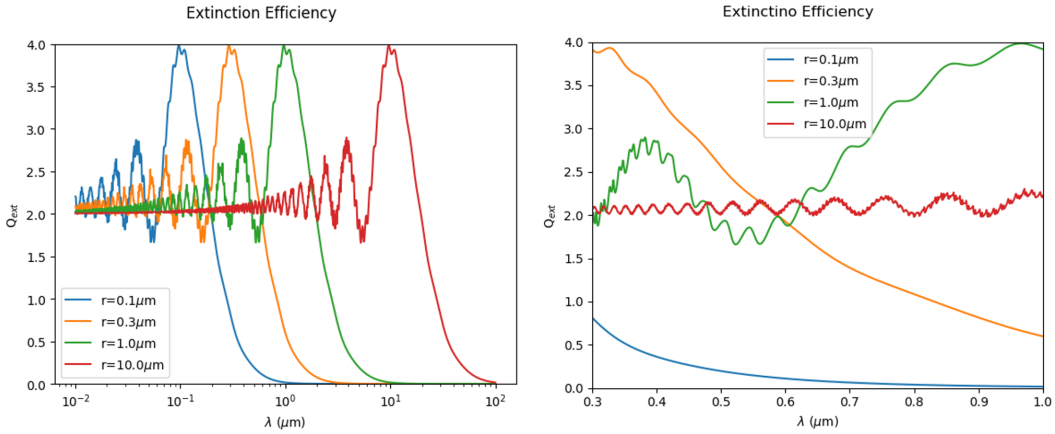

Figure 2. Adapted from Petty (2004) Fig. 12.5. Extinction Efficiency with respect to wavelength, with varying particle radius. Complex refractive index $m = 1.33 + 0j$. The left and right panels show logarithmic and linear scales, respectively.

in Q_e can be as significant as orders of magnitude. This observation first hints at how particle size can impact the spectral feature of the material.

2.2.2. *1D Climate Simulation with PCM_LBL*

PCM_LBL is a 1D radiative-convective model that simulate the climates of planets. It solves for the radiative transfer and thermodynamic structure of a planetary atmosphere.

In this report, the scattering version of PCM_LBL is modified to take in the scattering parameters calculated in section 2.2.1, namely the extinction coefficient β, the single scattering albedo ϖ, and the asymmetry parameter g. The shortwave scattering and absorption, as well as longwave absorption by the dust, are included.

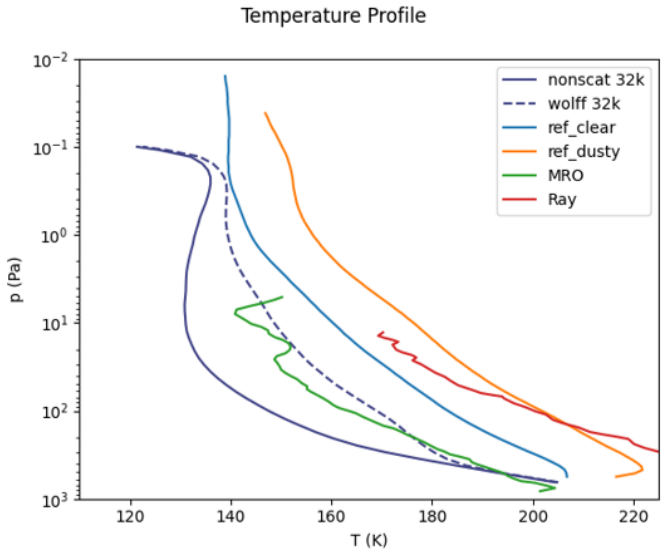

Figure 3. Equilibrium temperature profile calculated using PCM_LBL. `wolff` refractive index data and present Martian atmospheric conditions are applied, including the following parameters: $p_{surf} = 650.0\text{Pa}, g_{grav} = 3.73\text{m/s}^2, F_0 = 441\text{W/m}^2, \tau_{9.3\mu\text{m}} = 0.2$.

The equilibrium atmosphere profile calculated using the atmospheric condition for modern Mars and the `wolff` data for dust refractive index described in section 2.1 is shown in Fig. 3. The reference data (green line) comes from the MRO radio science data (Hinson et al. 2014). The PCM simulation results agree well with the MRO observational data.

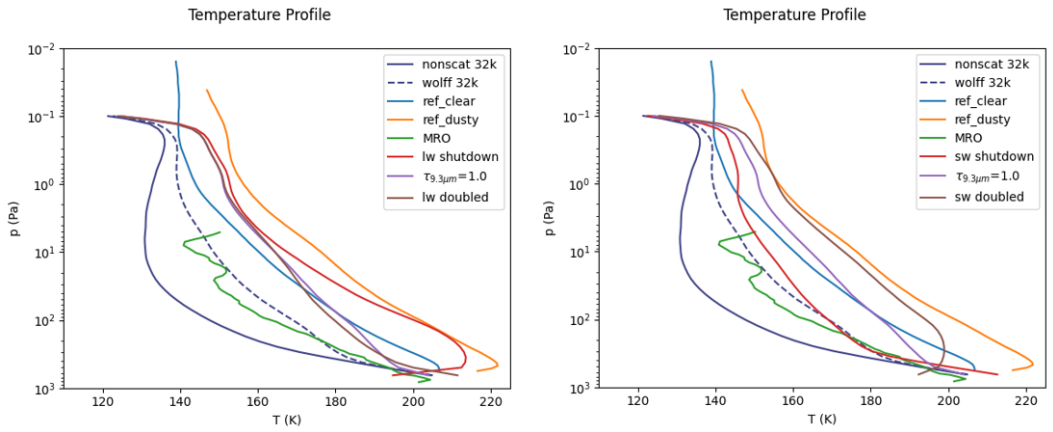

Figure 4. Test the PCM scattering module with different scattering configurations. The default optical depth corresponds to $\tau_{9.3\mu m} = 1.0$, which is exaggerated to see the effect of shortwave and longwave scattering more clearly. The left and right panels show the result with varying shortwave and longwave scattering intensity, i.e., shutdown, default, and doubled.

To further validate that the scattering module of the PCM is working, several test cases were performed. The results are shown in Fig. 4. The figure shows the effect of varying intensity of the shortwave and longwave scattering process on the atmospheric structure, especially near the surface. The trend is consistent with our expectation from physical intuition.

2.3. *Investigating Surface Reflectance Models*

2.3.1. *A Critical Analysis of the Shkuratov Model*

The description of the Shkuratov model can be found in Shkuratov et al. (1999).

The model uses a quasi-1D model to model the propagation of a light ray inside a particulate, layered medium. The model's basic assumptions are that the propagation can be separated into two parts: interacting with the interface and traveling inside the medium. The first one can be described with the Fresnel Equation, and the latter part is just Beer's Law, i.e., exponential decay.

The model first calculates the properties of traveling light interacting with a single particle. The light can either be directly reflected when it is incident from outside, or it can also penetrate into the particle. The model integrates the Fresnel equation in the upper and lower hemispheres to calculate the fraction of these two scenarios. The transmitting light in the particle then experiences internal reflection, each time having some probability that some portion of the light transmits outside the particle. The model deals with the internal reflection using also the Fresnel equation, but when dealing with the transmitted light from the internal reflection process, the authors made a bold assumption, saying that $W_i = \frac{1}{2}$ for $i > 2$, with W_i means the probability of light to be reflected after the i-th interaction with the interface. They argued that $W_2 = 0$ because light transmitted through a particle without internal reflections cannot be directed toward the source, which makes sense. However, they then claimed that, as a more detailed estimation of W_i is impossible, they further assumed that $W_i = \frac{1}{2}$ for $i > 2$, which is a questionable assumption without further justification.

After obtaining the reflecting properties of a single particle, the paper models the medium as layers, with each layer composed of such particles and spaces, thus including the effect of porosity as well. The paper then constructs a self-consistent equation describing the reflectance of this 1D-layered model to acquire the medium's final albedo.

Also, because this model came to an algebraic form of the albedo, it can also be used to retrieve the imaginary part of the refractive index, i.e., k, once the albedo and real part n are known.

However, although this model is self-consistent in the sense that retrieval of the result from the forward model can return the input values, it fails to comply with experimental data. Even the figure from the paper cannot be reproduced by the data and method from the same paper, as shown in Fig. 5. In fact, the method described in the paper only applies to media with small k, because once k reaches 10^{-2} order, its effect in the Fresnel equation is not negligible. The paper, however, claims to have retrieved k to the order of 10^0 (see Fig. 5), which further reduces the paper's credibility.

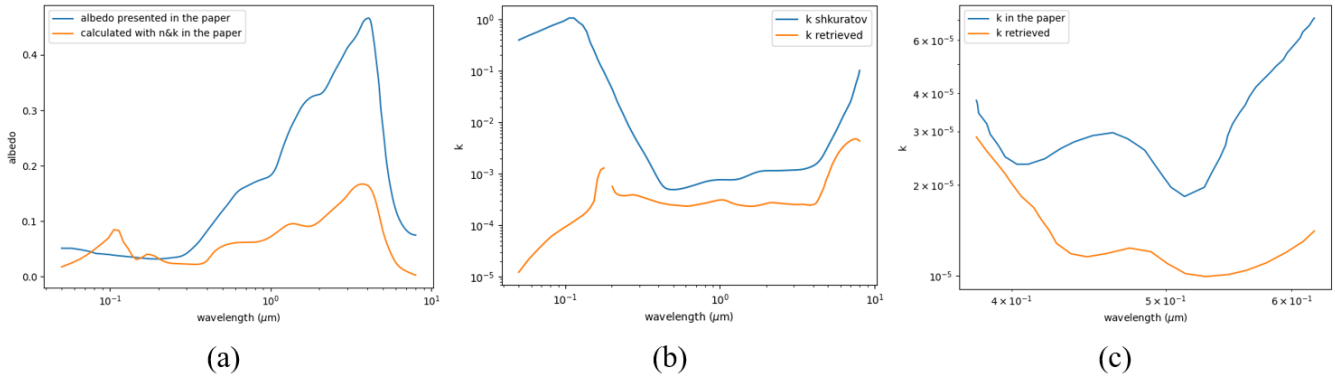

Figure 5. Attempts to reproduce figures from Shkuratov et al. (1999). (a) Forward model albedo result using n, k in Fig. 5 in Shkuratov as input, which differs from the albedo in the same figure in the paper. (b) Retrieval result using A, n as input. The retrieval result from the paper shows k as large as 10^0, which contradicts the basic assumption (k is small so that it can be neglected in the Fresnel equation). (c) Retrieval result using A, n from Fig. 4 in Shkuratov et al. (1999), the result differs from the paper even for small k.

2.3.2. *Hapke model*

Hapke's model is described in his book Hapke (2012).

Hapke illustrated that the propagation of light in a particulate medium can be described using radiative transfer theory. By doing so, the model neglects the interaction between adjacent particles and considers every particle to be scattering independently. For the simplified case, he assumes the particles to be isotropic scattering, which is the Isotropic Multiple Scattering Assumption (IMSA). There is also an expression for hemispherical reflectance including the anisotropic effect, i.e., Modified Isotropic Multiple Scattering Assumption (MIMSA). The expressions for hemispherical reflectance in these two models are as follows.

$$r_h^{IMSA}(i) = \frac{1-\sqrt{1-\varpi}}{1+2\mu_0\sqrt{1-\varpi}} \tag{1}$$

$$\begin{aligned} r_h^{MIMSA}(i) =& 1-\sqrt{1-\varpi}H(\mu_0) + b_1\left\{\mu_0 - \frac{1}{2}\left[H(\mu_0)-1\right]\right\} \\ &\times\left\{\frac{\varpi}{2}\left[\frac{1}{2}-\mu_0+\mu_0^2\ln\frac{1+\mu_0}{\mu_0}\right] + \frac{1}{2}\left[\frac{1}{H(\mu_0)}-\sqrt{1-\varpi}\right] - \frac{\varpi}{4}\left[1-\mu_0\ln\frac{1+\mu_0}{\mu_0}\right]\right\} \end{aligned} \tag{2}$$

ϖ is the single scattering albedo, which is calculated using the method described in 2.2.1. $\mu_0 = \cos i$ is the cosine value of the incident angle, $H(x)$ is Chandrasekhar's H function, and b_1 is the first-order Legendre coefficient of the phase function, which can be found to be equal to $b_1 = 3g$.

Fig. 6 shows the albedo results from the Hapke and semi-infinite cloud models (Petty 2004). The general spectral features and the qualitative dependence of albedo on particle sizes are consistent with Paragas et al. (2025). It is also worth noting that a relatively simple semi-infinite model can produce results similar to those of the Hapke model.

Although the Hapke model can produce seemingly reasonable results and is widely used in the field, there exists criticism against it, most notably from Mishchenko (1994) and Shkuratov et al. (2012). Hapke responded to these criticisms, admitting that his model is far from a rigorous solution of Maxwell's equations, but a useful model containing assumptions and approximations. Thus, it would be ideal to verify the model using known data, including observational data from Earth and laboratory measurements.

2.3.3. *Mishchenko model*

We investigated the model developed by Mishchenko et al. (1999) to calculate Martian dust's bidirectional reflectance function (BRF), which can be integrated over the hemisphere to get the hemispherical reflectance. The model is designed for optically semi-infinite, homogeneous particulate layers and works by iteratively solving Ambartsumian's nonlinear integral equation, for which no explicit analytical solution exists.

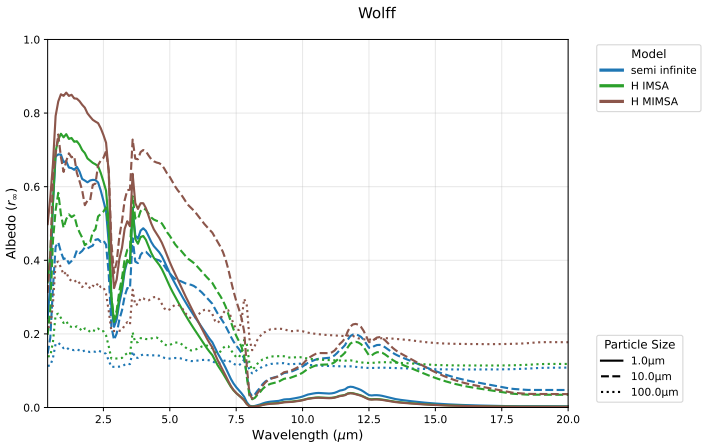

Figure 6. Calculated albedo for `wolff` data. Results from three models for three different particle effective radii are shown: (a) Semi-infinite cloud model; (b) Isotropic version of Hapke model; (c) Modified Hapke model.

Upon testing the publicly available FORTRAN code, we encountered two primary issues. First, when using `wolff` optical data for dust particles of radius $r = 1\mu$m, the model yielded extremely low albedo values, contradicting known measurements of the Martian surface. Second, the code failed to execute for particles of radius $r = 10\mu$m, resulting in a runtime error. This was surprising, as the author's original paper successfully demonstrates results for particles of a similar size.

We successfully replicated the benchmark case provided on the author's website, which indicates that the core of the code is likely functional. Therefore, we suspect the problems stem from specific configurations required by our input parameters. However, due to the lack of detailed documentation, we concluded that debugging the code would be too time-intensive and decided to pursue alternative methods.

3. DISCUSSION

3.1. *Effect of particle radius on reflectance*

As indicated in section 2.2.1, the particle size can significantly impact the optical properties of particles within a given wavelength range.

Fig. 7 can be used to illustrate further how particle size affects the albedo. From the figure, we can see that for the visible band and typical range of k, r_{eff} ($k < 10^0, r_{eff} > 10^0\mu$m), we generally have the albedo larger for smaller k and smaller r_{eff}. The impact of particle size is of a comparable order of magnitude to that of k. This stresses the importance of determining the radius distribution of the regolith in practical calculations.

3.2. *Color results from Hapke model and colorimetry theory*

This section serves more as an intuitive visualization rather than rigorous scientific findings. In this section, we adopt the theory from colorimetry to build a connection between the spectral reflectance of visible light and the color perceived by human eyes.

Human eyes have three types of cone cells, each of which has a distinct spectral response function to lights of different wavelengths. The response functions of these three cone cells are $L(\lambda), M(\lambda), S(\lambda)$, representing long to short wavelength. By integrating the spectrum using these corresponding functions as weighing functions, we can get the so-called LMS values, which can be converted into RGB values that can be displayed on a screen.

Fig. 8 shows the colors calculated for various samples with different particle sizes. Notably, the calculated color for hematite is consistent with the streak color of real hematite samples.

3.3. *Other factors affecting reflectance of planetary regolith*

The reflectance of planetary regoliths is governed by complex factors extending far beyond simple particle size and bulk chemical composition. The foundational assumptions of many radiative transfer models, such as those employing Mie theory, often diverge significantly from the physical reality of regolith.

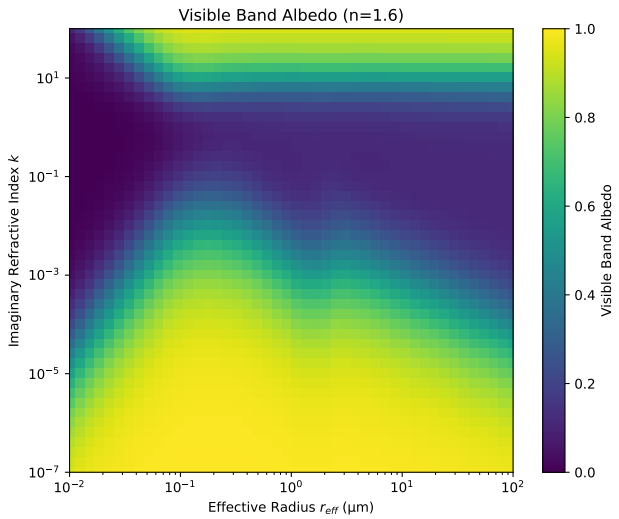

Figure 7. Albedo with varying k and r_{eff}. k represents the imaginary part of the refractive index and is assumed to be constant over the spectral range, r_{eff} is the effective radius of log-normal distributed particle sizes. The real part of the refractive index n is also assumed to be a constant value $n = 1.6$ over the spectral range. The albedo is integrated over the spectral range using the blackbody radiation function at $T = 5870K$ as a weighing function.

Figure 8. Color obtained from colorimetry theory. The reflectance is calculated using the Hapke model described in section 2.3.2.

First, these models typically assume homogeneous, spherical particles, whereas actual regolith grains are irregularly shaped, inhomogeneous agglutinates. The properties of the particle surface, for example, coatings, are particularly crucial. This is strongly supported by the findings in Pieters et al. (1993), which showed that the spectral features of fine-grained lunar soil could not be replicated by simply grinding larger grains, highlighting the importance of surface-altering processes. Furthermore, mineralogy, distinct from bulk chemistry, plays a vital role, as do trace amounts of substitutional cations, which can create significant absorption features.

Second, independent scattering is a nearly universal assumption in these models. This approximation breaks down in a densely packed medium like regolith, where near-field interactions and spatial correlations between particles

become significant and can alter the single-scattering properties. An example of such a phenomenon is frustrated total internal reflection via evanescent waves between closely spaced particles. Although Mishchenko (1994) attempted to incorporate these collective effects, for instance, through a static structure factor, such approaches often rely on simplifying assumptions. A truly rigorous solution—solving Maxwell's equations for the entire many-body system—remains computationally intractable, making accurately modeling dense particulate media a major unsolved problem in the field.

4. CONCLUSION AND FUTURE WORK

4.1. *Conclusion*

In this report, we explored the radiative effects of dust on the climate of early Mars through a dual approach: modeling the scattering by airborne dust and the reflectance of surface regolith.

We have successfully established and validated a computational framework that couples Mie scattering theory with the PCM_LBL 1D radiative-convective climate model for airborne dust. The validation runs for present-day Mars show good agreement with observational data, confirming the reliability of our tools for simulating the climatic impact of atmospheric dust.

The investigation into surface reflectance properties proved more complex. After critically analyzing several theoretical models, we identified the Hapke model as the most practical, although imperfect, tool for this study. Our modeling with the Hapke framework yielded a crucial insight: the surface albedo is not only dependent on the intrinsic optical properties of the material (i.e., the imaginary part of the refractive index, k), but is also strongly influenced, to an equivalent degree, by the particle size distribution. This finding underscores that physical properties can be as important as chemical composition in determining a planet's radiative balance.

However, this work also highlights the inherent limitations of current idealized models. Mie theory and the Hapke model rely on simplifying assumptions, such as homogeneous, spherical particles and independent scattering. As our discussion pointed out, the fundamental physical properties of planetary regolith are far more intricate, involving factors like mineralogy, particle shape, surface texture, coatings, and collective scattering effects in dense media.

In summary, this project has not only built the necessary numerical tools to investigate the radiative impact of dust on Mars but, more importantly, has revealed the profound complexity of accurately characterizing dust's optical properties. Our findings demonstrate that relying on bulk composition alone is insufficient. A comprehensive understanding requires a holistic approach that integrates the mineralogical, physical, and textural properties of the dust. This conclusion has significant implications for studies of both early Mars and terrestrial exoplanets.

4.2. *Future work*

4.2.1. *Comparison with Earth observation & lab measurements*

The Hapke model is widely accepted in the planetary science community, yet the most common use is to determine the composition of mixed samples given the spectra of the mixture and the components. As an empirical model, its forward model from single scattering properties to macroscopic albedo and the corresponding backward model still need verification with constraints from real data.

One beneficial verification comes from the model's application to Earth's environment, such as the reflectance of the Saharan desert. This verification, however, faces some difficulties due to data availability. As the Hapke model is a forward model that requires both refractive index and particle size data to predict albedo, it is hard to find such data. Paragas et al. (2025) has offered an invaluable database of measured albedo for several standard terrestrial planet rock samples. It clearly illustrates the importance of surface texture to its reflection and emission properties. However, the paper only provides results for three different kinds of textures, i.e., slab, crushed, and powder. As the Hapke model can predict the quantitative relation between surface reflectance and particle size distributions, as seen in Fig. 6, obtaining measurement data for higher particle size resolutions is desirable. This involves sample preparation, including grinding and sieving the sample to get the expected particle size range, and reflectance measurement using a spectrometer. This enables us to evaluate the Hapke model's ability to accurately account for the dependence of reflectance on particle size, which is crucial in determining surface albedo.

4.2.2. *Implication on early Mars*

Using broadband albedo rather than spectral albedo is standard practice in climate modeling. For Mars studies, the value of the broadband albedo is often assigned to a characteristic value, such as 20%. However, with the change of

surface properties over geological time, it is unclear how much the surface albedo of early Mars differed from the typical value for present-day Mars. Our motivation for this project was that the change in oxidation state determines the change in optical properties of the dust, which then has different climate impacts. However, as we have demonstrated in section 3.1, the particle size alone can be as important as chemical composition in determining the reflectance. This requires us to synthesize the existing evidence and give a more rigorous description of the early Martian planetary albedo. This includes putting a physical constraint on the particle size distribution, taking potential atmospheric, fluvial, and space weathering into account.

Also, changes in dust's physical and chemical properties can significantly impact airborne dust. Changes in single scattering properties can lead to different radiative forcing in the atmosphere. Changes in size distribution and shape not only impact the single scattering features but can also alter the dust's aerodynamic properties, leading to different lifting and deposition behavior. All these processes can contribute to the climate effect of dust on early Mars.

4.2.3. *Implication on exoplanets*

The topic of optical properties of particulate material explored in this report has broader implications beyond early Mars. The surface reflectance and emissivity depend on several aspects, as discussed in section 3.3, which makes the deduction from observed spectral data to a detailed description of the planetary surface very difficult. However, such knowledge is helpful when it comes to exoplanet characterization. For bare rock planets, the emission spectrum directly tells us information about their surface. It can also constrain the expected spectrum for bare rock planets with various surface types, thus guiding us to find anomalies that might imply the existence of an atmosphere. For example, Mansfield et al. (2019) used inferred high albedo to argue that within a given temperature range, no bare rock surface could present such high albedo, thus the existence of an atmosphere can be inferred.

APPENDIX

A. FRESNEL EQUATION

The fundamental interaction of light with matter, such as reflection and refraction at an interface, is quantitatively described by the Fresnel equations (Paschotta 2013). Derived from the Maxwell equations, these relations govern the behavior of electromagnetic waves at a smooth, planar boundary between two homogeneous, isotropic media with different refractive indices.

To apply the equations, the incident light's electric field is decomposed into two orthogonal polarization components: one parallel to the plane of incidence ($p-$polarized) and the other perpendicular to it ($s-$polarized). The Fresnel equations then provide the amplitude reflection coefficients:

$$\begin{cases} r_s = \frac{E_{r,s}}{E_{i,s}} = \frac{m_1 \cos\theta_1 - m_2 \cos\theta_2}{m_1 \cos\theta_1 + m_2 \cos\theta_2} \\ r_p = \frac{E_{r,p}}{E_{i,p}} = \frac{m_1 \cos\theta_2 - m_2 \cos\theta_1}{m_1 \cos\theta_2 + m_2 \cos\theta_1} \end{cases} \tag{A1}$$

Where m_1, m_2 are the complex refractive indices of the two media, and θ_1, θ_2 are the angles of incidence and refraction, respectively. The reflectance R, or the fraction of incident power that is reflected, is given by $R_s = |r_s|^2$ and $R_p = |r_p|^2$.

These equations reveal that the reflectance strongly depends on incidence angle, polarization state, and the optical constants of the materials. However, the Fresnel equations only apply to an optically flat surface where the height variations are much smaller than the wavelength of incident light. This highly ideal condition makes it insufficient for describing planetary regoliths. Like Mars, real surfaces are composed of particulate and rough materials, where complex phenomena such as multiple scattering between particles occur. Therefore, the Fresnel equations serve as a theoretical baseline, motivating the use of more sophisticated models like those of Shkuratov and Hapke discussed in section 2.

Nevertheless, the Fresnel equations can provide fundamental physical insights into the interaction between incident light and the interface. Fig. A1 shows the reflectance with respect to incident angle. Because the incident light is always natural light, which is unpolarized, the total reflectance is just $R = \frac{1}{2}(R_s + R_p)$. From the figure, we can see that for a small k value, the reflectance is very close to that of the $k = 0$ case. This can be explained by the following asymptotic relation:

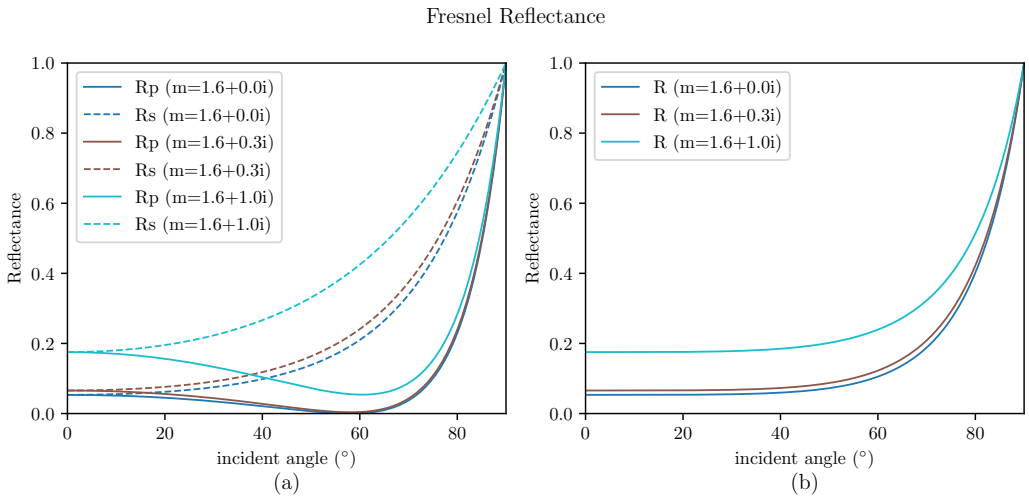

Figure A1. (a) The reflectance of $p-$ and $s-$ polarized incident light with respect to incident angle. The real part of the refractive index n is fixed to 1.6, the imaginary part k takes values of $0.0, 0.3, 1.0$. (b) As for (a), but for the total reflectance.

$$R(0^\circ) \simeq \left|\frac{n-1}{n+1}\right| \cdot \left[1 + \frac{4nk^2}{(n-1)^2(n+1)^2} + O(k^4)\right] \tag{A2}$$

For small k, the difference in reflectance caused by k is proportional to k^2, making it a reasonable approximation to neglect k in the reflectance when k is small.

It is also worth noting that the reflectance is larger with larger k, contrary to the intuition that reflectance should be smaller with larger k, since k corresponds to absorption in the medium. In fact, k corresponds to the absorption of light traveling inside the medium, but the difference in k between the media makes the electromagnetic wave harder to penetrate through the interface; thus, a larger k corresponds to increasing reflectance.

REFERENCES

Connour, K., Wolff, M. J., Schneider, N. M., et al. 2022, Icarus, 387, 115177, doi: 10.1016/j.icarus.2022.115177

Deguine, A., Petitprez, D., Clarisse, L., et al. 2020, Applied Optics, 59, 884, doi: 10.1364/AO.59.000884

Haberle, R. M., Clancy, R. T., Forget, F., Smith, M. D., & Zurek, R. W., eds. 2017, The Atmosphere and Climate of Mars (Cambridge University Press)

Hapke, B. 2012, Theory of Reflectance and Emittance Spectroscopy, 2nd edn. (Cambridge University Press)

Hinson, D. P., Asmar, S. W., Kahan, D. S., et al. 2014, Icarus, 243, 91, doi: 10.1016/j.icarus.2014.09.019

Lamy, P. L. 1978, Icarus, 34, 68, doi: 10.1016/0019-1035(78)90126-4

Liu, J., Michalski, J. R., Tan, W., et al. 2021, Nature Astronomy, 5, 503, doi: 10.1038/s41550-021-01303-5

Mansfield, M., Kite, E. S., Hu, R., et al. 2019, The Astrophysical Journal, 886, 141, doi: 10.3847/1538-4357/ab4c90

Mishchenko, M. I. 1994, Journal of Quantitative Spectroscopy and Radiative Transfer, 52, 95, doi: 10.1016/0022-4073(94)90142-2

Mishchenko, M. I., Dlugach, J. M., Yanovitskij, E. G., & Zakharova, N. T. 1999, Journal of Quantitative Spectroscopy and Radiative Transfer, 63, 409

Paragas, K., Knutson, H. A., Hu, R., et al. 2025, A New Spectral Library for Modeling the Surfaces of Hot, Rocky Exoplanets, arXiv, doi: 10.48550/arXiv.2502.04433

Paschotta, R. 2013, Fresnel Equations, RP Photonics Encyclopedia, RP Photonics AG, doi: 10.61835/tql"title="Thislinkwillreloadthecurrentpage.

Petty, G. W. 2004, in A First Course in Atmospheric Radiation. https://api.semanticscholar.org/CorpusID:129376785

Pierrehumbert, R. T. 2010, Principles of Planetary Climate (Cambridge University Press)

Pieters, C. M., Fischer, E. M., Rode, O., & Basu, A. 1993, Journal of Geophysical Research: Planets, 98, 20817, doi: https://doi.org/10.1029/93JE02467

Pollack, J. B., Toon, O. B., & Khare, B. N. 1973, Icarus, 19, 372, doi: 10.1016/0019-1035(73)90115-2

Shkuratov, Y., Kaydash, V., Korokhin, V., et al. 2012, Journal of Quantitative Spectroscopy and Radiative Transfer, 113, 2431, doi: 10.1016/j.jqsrt.2012.04.010

Shkuratov, Y., Starukhina, L., Hoffmann, H., & Arnold, G. 1999, Icarus, 137, 235, doi: 10.1006/icar.1998.6035

Wolff, M. J., Smith, M. D., Clancy, R. T., et al. 2009, Journal of Geophysical Research: Planets, 114, 2009JE003350, doi: 10.1029/2009JE003350

Wolff, M. J., Smith, M. D., Clancy, R. T., et al. 2006, Journal of Geophysical Research: Planets, 111, doi: https://doi.org/10.1029/2006JE002786